

Confocal imaging of Bim translocation to endoplasmic reticulum during DHA-induced ASTC-a-1 cell apoptosis

Min Chen (陈敏)¹, Yingying Lu (卢盈颖)¹, Tongsheng Chen (陈同生)^{1*}, and Junle Qu (屈军乐)²

¹MOE Key Laboratory of Laser Life Science & Institute of Laser Life Science, South China Normal University, Guangzhou 510631, China

²Key Laboratory of Optoelectronic Devices and Systems of Ministry of Education & Guangdong Province, Institute of Optoelectronics, Shenzhen University, Shenzhen 518060, China

*E-mail: chentsh@scnu.edu.cn

Received June 22, 2010

Bim, a proapoptotic member of Bcl-2 family, plays an important role in cell apoptosis. It is generally thought that Bim translocates to mitochondria in response to apoptotic stimuli. We use confocal microscopy to image the temporal-spatial dynamics of Bim during dihydroartemisinin (DHA) induced human lung adenocarcinoma (ASTC-a-1) cell apoptosis. Interestingly, we find that DHA induces Bim translocation to endoplasmic reticulum (ER) rather than mitochondria, implying that Bim-ER pathway might be involved in the DHA-induced ASTC-a-1 cell apoptosis.

OCIS code: 170.1530, 170.1790, 170.2655.

doi: 10.3788/COL20100810.0950.

Dihydroartemisinin (DHA), a semi-synthetic derivative of artemisinin, isolated from the traditional Chinese herb *Artemisia annua*, is recommended as a first-line anti-malarial drug with low toxicity. More recent studies including those from our laboratory have revealed that DHA can inhibit the growth of cancer cells through apoptotic pathway^[1,2]. However, the mechanism of apoptosis induced by DHA has not yet been elaborated clearly^[3,4].

Confocal microscopy imaging has been widely used to investigate the temporal-spatial dynamics of molecules in single living cells. The key feature of confocal microscopy is its ability to acquire in-focus images from selected depths, a process known as optical sectioning. Images are acquired point-by-point and reconstructed with a computer. In this letter, confocal imaging is performed on a confocal microscope system with C-Apochromat 40× (numerical aperture NA=1.3) and 100×(NA = 1.4) oil objectives (Carl Zeiss Inc., Germany). The system is equipped with a CO₂ pump (Carl Zeiss MicroImaging Inc., Germany) and a temperature regulator (Carl Zeiss MicroImaging Inc., Germany), which keep cells in the normal culture condition during imaging. Cells are maintained at 37 °C with 5% CO₂ in humidified chamber throughout the experimental process^[5]. The excitation wavelengths are 488 nm for green fluorescent protein (GFP) and 543 nm for er-RFP (encoding endoplasmic reticulum (ER) targeted red fluorescent protein (RFP)). The emission fluorescence channels were 500–550 nm for GFP and 560 nm long-pass for er-RFP^[6].

ER and mitochondria are two important cellular organelles in cell apoptosis^[7,8]. Bim, a BH₃-only protein, plays an important role in cell apoptosis^[9]. It is generally considered that Bim translocates to mitochondria in response to apoptosis stimuli^[10,11]. We use time-lapse confocal imaging to monitor the dynamics of Bim translocation during DHA-induced human lung adenocarcinoma (ASTC-a-1) cell apoptosis in single living cells. Contrary to our expectation, we find that it is the ER but not mitochondria that Bim translocates to during

DHA-induced ASTC-a-1 cell apoptosis.

Cell counting kit (CCK-8) assay is a sensitive non-radioactive colorimetric assay for determining the number of viable cells in cell proliferation and cytotoxicity assays^[12,13]. The effect of DHA on cell viability was assessed using CCK-8. Cells were suspended at a final concentration of 5×10^3 cells/well and cultured in 96-well flatbottom microplate. After exposure to DHA, CCK-8 (10 μ L) mixed with culture medium (90 μ L) was added to each well of a 96-well flatbottom microplate, and the plate was incubated for 1 h at 37 °C in a humidified 5% CO₂ incubator. Viable cells were counted by absorbance measurements at 450 nm using auto microplate reader (infinite M200, Tecan, Austria). The value of optical density (OD) at 450 nm was inversely proportional to the degree of cell apoptosis. All experiments were performed in triplicate on three separate occasions^[12,13]. As shown in Fig. 1, the proliferation of the ASTC-a-1 cells was inhibited in a time-dependent manner after treatment with 20 μ g/mL of DHA for different time (0, 12,

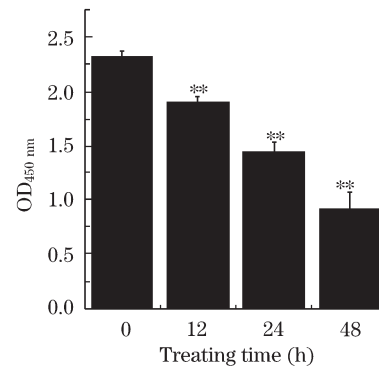


Fig. 1. Cell viability measured by CCK-8 assay. Cells are seeded into 96-well flatbottomed microplate and incubated with DHA for various time (0, 12, 24, and 48 h). Data analyzed with SPSS10.0 software are expressed as mean \pm SD. Well number $n = 4$ for all CCK-8 assay. ** $P < 0.01$, compared with control. SD: standard deviation.

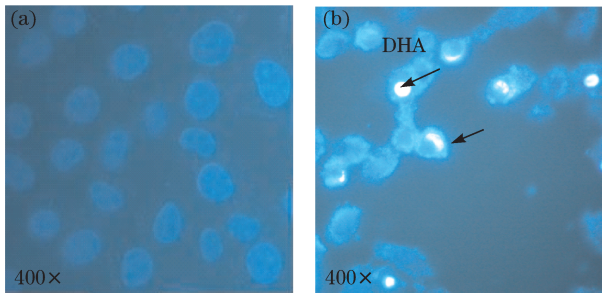


Fig. 2. Hoechst 33258 images of cells. Cells are treated with 20 $\mu\text{g}/\text{mL}$ of DHA for 48 h. Nuclear morphology is examined by fluorescence microscope. (a) Control cells show dispersive light blue nucleus and intact structure; (b) DHA-treated cells show cell shrinkage, chromatin condensation, and margination in the nucleus.

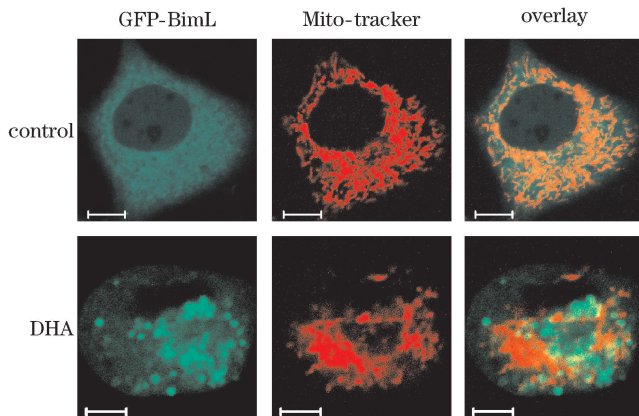


Fig. 3. Bim does not translocate to mitochondria under the treatment of DHA in ASTC-a-1 cells. Cells are treated with 20 $\mu\text{g}/\text{mL}$ of DHA for 24 h. Dynamics of Bim are examined by fluorescence microscope. Control cells show Bim uniform distribution. DHA-treated cells show Bim translocation, but no co-localization with mitochondria. The scale bar is 5 μm .

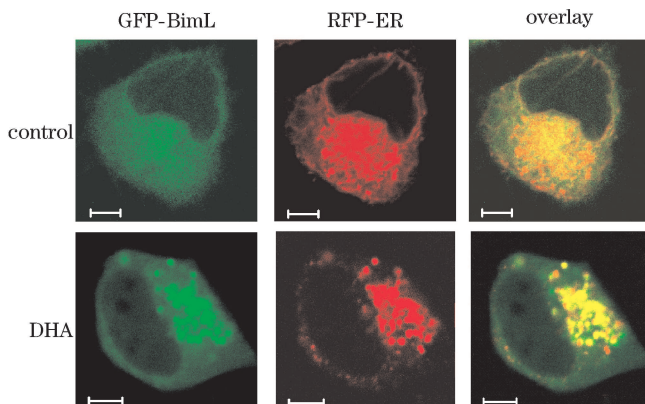


Fig. 4. Bim translocates to ER under the treatment of DHA. Cells are treated with 20 $\mu\text{g}/\text{mL}$ of DHA for 24 h. Dynamics of Bim are examined by fluorescence microscope. Control cells show the uniform distribution of Bim. DHA-treated cells show the co-localization between Bim translocation and ER. The scale bar is 5 μm .

24, and 48 h). These results show that DHA effectively exerts cytotoxicity on cells in a time-dependent manner.

To determine the form of DHA-induced cell death, we

used Hoechst 33258 staining to image the morphology of deoxyribonucleic acid (DNA). Morphological changes and DNA fragmentation are considered as the major cytopathologic hallmarks of the apoptotic process^[1]. Hoechst 33258 is one of the blue fluorescent dyes that can penetrate the cell membrane freely. Cells were grown on the coverslip of a 35-mm chamber. After being treated with 20- $\mu\text{g}/\text{mL}$ DHA for 24 h, the cells were washed with phosphate buffer saline (PBS) three times and incubated with 1- $\mu\text{mol}/\text{L}$ Hoechst 33258 mixed with culture medium (499 μL) for 20 min at room temperature in the dark. Cells were then washed three times with PBS and observed under a laser scanning confocal microscope (LSM510/ConfoCor2, Zeiss, Germany) (Fig. 2). The images of Hoechst 33258 were recorded using a digital camera (Nikon, Japan) with the resolution of 1280 \times 1280 pixels. The nuclei in normal cells exhibited diffused staining of the chromatin (Fig. 2(a)). However, after exposure to 20- $\mu\text{g}/\text{mL}$ DHA for 48 h, the cells underwent typical morphologic changes of apoptosis such as chromatin condensation, margination, and shrunken nucleus (Fig. 2(b)), the arrows point to cells displaying nuclear fragmentation). These results suggest that the form of cell death induced by DHA is apoptosis.

Although we have certificated the form of cell death induced by DHA was apoptosis, the mechanism has not yet been elaborated clearly. To investigate the function of Bim in DHA-induced apoptosis, we used confocal microscopy to image the temporal-spatial dynamics of Bim during DHA-induced cell apoptosis. Generally, it is reported that Bim translocates to mitochondria to promote apoptosis^[10,11]. In order to determine whether Bim translocated to mitochondria, we used confocal microscopy to image the temporal-spatial distributions of Bim (Fig. 3). Cells were grown on the coverslip of a 35-mm chamber for 24 h, transfected with GFP-BimL plasmids for 36 h, then treated with 20- $\mu\text{g}/\text{mL}$ DHA for 24 h, and stained with Mitotracker dyes, a mitochondria specific marker. Subsequently, cells were examined using a laser scanning confocal microscope (LSM510/ConfoCor2, Zeiss, Germany). Although DHA induced a significant Bim translocation as our expectation, it was disappointed that Bim did not translocate to mitochondria in DHA-induced cell apoptosis (Fig. 3). To assess whether Bim translocated to ER during DHA-induced apoptosis, cells were cotransfected with er-REP and GFP-BimL plasmids for 48 h, subsequently treated with 20- $\mu\text{g}/\text{mL}$ DHA for 24 h, and then examined using a laser scanning confocal microscope. Surprisingly, the overlay image shows that DHA-induced Bim translocates to ER (Fig. 4), implying that Bim might play a role in DHA-induced apoptosis via ER pathway.

Our data show that DHA induces translocation of Bim to ER. It is likely that Bim accumulates on ER and acts as a trigger for caspase-12 activation, thus bringing about the ER stress-induced apoptosis^[14]. It is also likely that Bim translocates to ER, and acts as a trigger for Bax/Bak activation, then leads to the release of Ca^{2+} from ER, which stimulates the release of mitochondrial cytochrome c^[15,16]. However, the exact molecular mechanism needs to be further explored. We will make further research to assess the function of Bim in DHA-induced cell apoptosis.

In conclusion, to our knowledge, we for the first time find that DHA induces Bim translocation to ER rather than mitochondria, implying that Bim-ER pathway might be involved in the DHA-induced ASTC-a-1 cell apoptosis. But the exact mechanism needs to be further investigated.

This work was supported by the National Natural Science Foundation of China (Nos. 31071218 and 60627003) and the Natural Science Foundation of Guangdong Province (Nos. 8151063101000031 and 9251063101000009).

References

1. Y.-Y. Lu, T.-S. Chen, J.-L. Qu, W.-L. Pan, L. Sun, and X.-B. Wei, *J. Biomed. Sci.* **16**, 16 (2009).
2. Y.-Y. Lu, T.-S. Chen, X.-P. Wang, J.-L. Qu, and M. Chen, *FEBS. Lett.* doi:10.1016/j.febslet.2010.08.014 (2010).
3. J.-J. Lu, L.-H. Meng, U. T. Shankavaram, C.-H. Zhu, L.-J. Tong, G. Chen, L.-P. Lin, J. N. Weinstein, and J. Ding, *Biochem. Pharmacol.* **80**, 22 (2010).
4. A. E. Mercer, J. L. Maggs, X.-M. Sun, G. M. Cohen, J. Chadwick, P. M. O'Neill, and B. K. Park, *J. Biol. Chem.* **282**, 9372 (2007).
5. X. Gao, D. Xing, L. Liu, and Y. Tang, *J. Cell. Physiol.* **219**, 535 (2009).
6. Y. Zhang, D. Xing, and L. Liu, *Mol. Boil. Cell* **20**, 3077 (2009).
7. H. Shiraishi, H. Okamoto, A. Yoshimura, and H. Yoshida, *J. Cell. Sc.* **119**, 3958 (2006).
8. E. V. Pavlov, M. Priault, D. Pietkiewicz, E. H. Y. Cheng, B. Antonsson, S. Manon, S. J. Korsmeyer, C. A. Mannella, and K. W. Kinnally, *J. Cell. Biol.* **155**, 725 (2001).
9. K.-J. Yin, C. Y. Hsu, X.-Y. Hu, H. Chen, S.-W. Chen, J. Xu, and J.-M. Lee, *J. Neurosci.* **26**, 2290 (2006).
10. T. Tong, J. Ji, S. Jin, X. Li, W. Fan, Y. Song, M. Wang, Z. Liu, M. Wu, and Q. Zhan, *Mol. Cell. Biol.* **25**, 4488 (2005).
11. N. R. Khawaja, M. Carre, H. Kixacic, M. A. Esteve, and D. Braguer, *Mol. Pharmacol.* **74**, 1072 (2008).
12. J. Zhang, D. Xing, and X. Gao, *J. Cell. Physiol.* **217**, 518 (2008).
13. F. Zhou, D. Xing, S. Song, Z. Ou, and W. Chen, *Chinese J. Lasers (in Chinese)* **36**, 2676 (2009).
14. N. Morishima, K. Nakanishi, K. Tsuchiya, T. Shibata, and E. Seiwa, *J. Biol. Chem.* **279**, 50375 (2004).
15. E. Szegezdi, S. E. Logue, A. M. Gorman, and A. Samali, *Embo. Rep.* **7**, 880 (2006).
16. Y. Zhang, D. Xing, and L. Liu, *Chinese J. Lasers (in Chinese)* **36**, 2609 (2009).